Fast-response Liquid Crystals for AR and Head-Up Displays

Yannanqi Li,[1] Yuge Huang,[1] Haruki Ooishi,[2] Kifumi Yoshidaya,[2] and Shin-Tson Wu[1]
[1]College of Optics and Photonics, University of Central Florida, Orlando FL
[2]DIC Corporation, Tokyo, Japan

Abstract
Two nematic liquid crystal mixtures with high birefringence, modest dielectric anisotropy, relatively low viscosity, and wide nematic range (-40°C ~105°C) are developed and their physical properties evaluated. When used in reflective LCoS panels, the average response time is 2.37 ms for 2π phase modulation and ~1ms for amplitude modulation. Potential applications for AR and head-up displays are emphasized.

Author Keywords
Fast response time; Liquid crystal on silicon; Augmented Reality; Head-up displays.

1. Introduction

Liquid-crystal-on-silicon (LCoS) has been widely used in augmented reality (AR) displays, such as Google Glass, HoloLens, and Magic Leap one, and vehicular head-up displays (HUDs) due to its low power consumption, high brightness, and high-resolution density [1-4]. Both amplitude modulation and phase modulation can be realized with LCoS, depending on the LC alignment. For amplitude modulation, reflective mixed-mode twist nematic (MTN) cell [5] and vertical alignment (VA) mode [6] are two common choices. For phase modulation, 2π phase change and 240 Hz refresh rate are highly desirable. A faster response time enables field sequential color operation. By eliminating the spatial color filters, both optical efficiency and resolution density are tripled. Another constraint for LCoS is that its operating voltage should be lower than 6 V [7].

To achieve fast response time for LCoS phase modulator, the simplest approach is to develop high birefringence (Δn) LCs with large dielectric anisotropy (Δε) and low viscosity. High Δn enables a thinner cell gap to achieve 2π phase change, which in turn leads to a faster response time. Large Δε helps to lower the operating voltage, but the tradeoff is increased viscosity. Therefore, there are compromises while optimizing the LC parameters.

In this paper, we report two LC mixtures which exhibit high birefringence (Δn≈0.24), modest dielectric anisotropy (Δε≈8), and wide nematic range (–40°C ~105°C). High Δn enables the use of thin cell gap (d=1.67 μm) to obtain 2π phase change and fast response time, especially the average phase-to-phase (PTP) response time (~2.37 ms). Meanwhile, a reasonably large $\Delta\varepsilon$ helps to lower the operating voltage to 5V. Finally, wide nematic range helps tolerate the harsh environment for vehicular displays.

2. Material characterization

Here, two new liquid crystal mixtures are denoted as RDP-A4869 and RDP-A4870, abbreviated as UCF-1 and UCF-2, respectively. Their physical properties are listed in Table 1. The measurement was conducted at 25°C. We measured the clearing point (Tc) and melting point (Tm) by using Differential Scanning Calorimetry (DSC, TA instruments Q100). High clearing point is crucial for vehicular head-up displays. The dielectric anisotropy was measured by a multi-frequency LCR meter HP-4274. A relatively large dielectric anisotropy helps to lower the threshold voltage V_{th} $=\pi\sqrt{K_{11}/\Delta\varepsilon}$, and the operating voltage is proportional to V_{th}. We also measured the rotational viscosity and splay, twist, and bend elastic constant through transient current method by autronic-MELCHRS LCCS107. Low visco-elastic constant contributes to faster response time since is linearly proportional to γ_1/K_{11}. The LC resistivity determines the voltage holding ratio (VHR). In LCoS displays, high frame rate helps to relax the requirement in VHR. In this case, the LC resistivity is usually set to be 10^{12} Ω·cm. Our LC resistivity (1.2×10^{12}) satisfies the requirement for LCoS displays.

Table 1. Measured physical properties of UCF-1 and UCF-2 at T=25°C.

LC mixtures	UCF-1	UCF-2
T_c (°C)	104.5	105.7
T_m (°C)	< -40	< -40
Δn@589 nm	0.242	0.240
$\Delta\varepsilon$ @1 kHz	7.53	9.16
$\varepsilon_\perp$ @1 kHz	3.42	3.66
γ_1 (mPa·s)	141	148
K_{11} (pN)	12.7	13
K_{22} (pN)	8.0	8.8
K_{33} (pN)	17.3	18
Resistivity (Ω·cm)	1.2×10^{12}	1.2×10^{12}

2.1 Birefringence

To achieve 2π phase change, higher birefringence enables a thinner cell gap (d) to be used. Small cell gap leads to faster response time, which is proportional to d^2. To measure Δn at different temperatures, we first injected each LC mixture into a commercial homogenous cell with cell gap d~5 μm. The pretilt angle of the rubbed polyimide alignment layers is about 3°C. Then the cell was fixed on a Linkam heat stage controlled by TMS94 Temperature Programmer and sandwiched between two crossed polarizers. The birefringence at each temperature was obtained from the measured phase retardation by applying 1kHz square-wave AC voltage to the LC cell. Figure 1(a) depicts the temperature-dependent birefringence at λ=632.8 nm (He-Ne laser). The dots represent the measured data and the solid line is the fitting curve with Haller's semi-empirical equation [8]:

$$\Delta n = \Delta n_0 S = \Delta n_0 \left(1 - T / T_c\right)^{\beta}. \quad (1)$$

Here, the birefringence Δn_0 is extrapolated at T=0, β is a material constant and S is the order parameter. The obtained Δn_0 and β values are listed in Table 2.

For a working LCoS device, the operating temperature is about 40°C because of the thermal effect from the CMOS backplane and illumination light. Therefore, we measured the wavelength dispersion at 40°C to investigate the electro-optical performances at RGB colors. In experiment, He-Ne laser (λ=632.8 nm) and a tunable Argon ion laser (λ=457 nm, 488 nm and 514 nm) were used as probing light sources. The obtained results are shown in Figure 1(b), where dots indicate measured data and solid lines are the theoretical fitting curves with the single-band birefringence dispersion equation [9]:

$$\Delta n = G\frac{\lambda^2\lambda^{*2}}{\lambda^2-\lambda^{*2}}, \quad (2)$$

where G is a proportionality constant and λ* is the mean resonance wavelength. From Eq. (2), birefringence at the RGB wavelengths we want can be calculated. At λ=633 nm and 40°C, the Δn of [UCF-1, UCF-2] is [0.226, 0.224], respectively. The obtained G and λ* values are also listed in Table 2.

2.2 Visco-elastic coefficient

Low visco-elastic coefficient contributes to fast response time. By measuring the transient decay curves of two LC mixtures, we can obtain the visco-elastic constant γ_1/K_{11} which is highly dependent on the temperature. Figure 1(c) depicts the γ_1/K_{11} at different temperatures, in which the dots represent the measured data. The solid lines represent fitting curves with following equation [10]:

$$\frac{\gamma_1}{K_{11}} = A\frac{\exp\left(E_a/k_BT\right)}{\left(1-T/T_c\right)^{\beta}}. \quad (3)$$

In Eq. (3), A is a proportionality constant, E_a is the activation energy and k_B is the Boltzmann constant. From Eq. (3) and Fig. 1(c), we could see that γ_1/K_{11} decreases exponentially as the temperature increases. At 40°C, the γ_1/K_{11} of [UCF-1, UCF-2] is [6.4, 6.8] ms/μm^2, respectively. The fitting parameters A and E_a are included in Table 2.

Table 2. Fitting parameters obtained from Eqs. (1)-(3)

LC mixture	UCF-1	UCF-2
Δn_0	0.308	0.306
β	0.174	0.177
G @40°C (μm^{-2})	3.17	3.06
λ* @40°C (μm)	0.247	0.248
A (ms/μm^2)	2.9×10^{-4}	3.36×10^{-4}
E_a (meV)	264	260

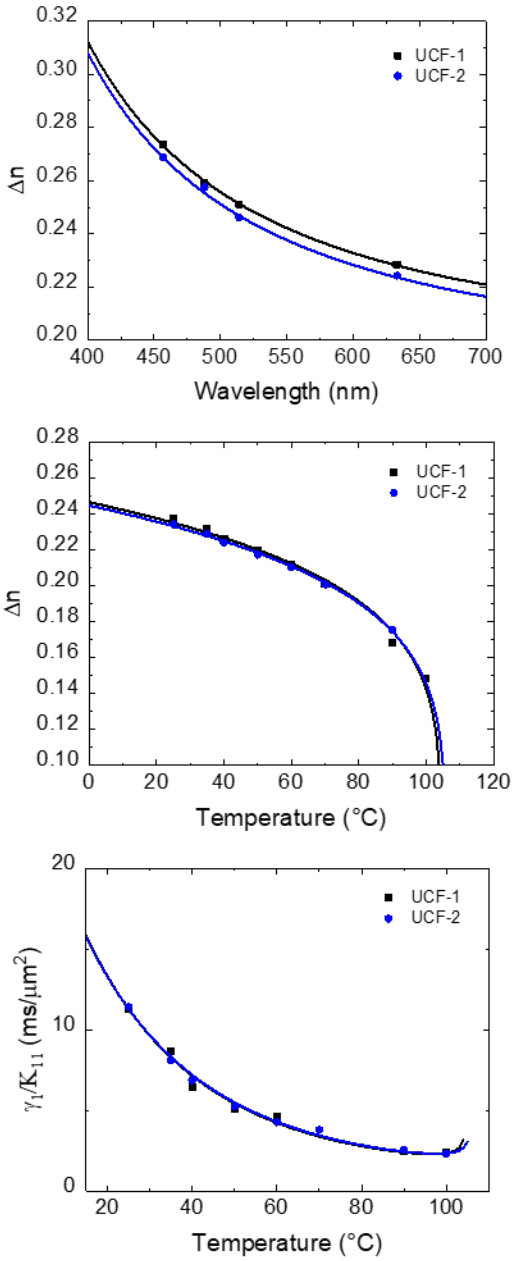

Fig. 1. (a) Temperature dependent birefringence at λ=633 nm and 1 kHz. (b) Wavelength dependent birefringence at T=40°C. (c) Temperature dependent visco-elastic coefficient at λ=633 nm. Dots are experimental data and solid lines are fitting curves with Eqs. (1)-(3).

3. Device performance

3.1 Grayscale phase response time

To study the phase-to-phase (PTP) response time of our LC device, we divided the VT curve into eight gray levels equally to represent the full phase tuning range as listed in Table 3. Here, we chose UCF-2 as an example for this study because of its better electro-optical performance. In experiment, we prepared a transmissive homogenous cell with cell gap d~3.33 μm and measured its response time between two phase levels in the transmissive mode. The experimental results as measured at 40°C

are listed in Table 4. The response time of an LC cell is proportional to d^2. In a reflective LCoS device, the response time is 4x faster than the measured one in transmissive mode. Therefore, for a 1.67-μm reflective LCoS panel, the extrapolated average PTP rise time is 1.53 ms and decay time is 0.84 ms. Therefore, for $V_{2\pi} = 4.54\ V$, the total average PTP response time is 2.37 ms which enables 240 Hz frame rate. Here we need to mention that the thinnest cell gap is 3.33 μm for transmissive mode in our lab. Since 2π phase change can be obtained by only 4.54 V which is far lower than the 6V limit, we can sacrifice the operating voltage to get faster response time by using a thinner cell gap.

Table 3. The corresponding operating voltage for selected nine phase levels between 0-2π. The transmissive homogenous cell gap is d=3.33 μm.

Phase level	Phase change (π)	Voltage (V)
1	0	0
2	0.25	1.55
3	0.5	1.76
4	0.75	1.97
5	1	2.22
6	1.25	2.53
7	1.5	2.88
8	1.75	3.4
9	2	4.54

Table 4. Measured phase-to-phase (PTP) response time at λ=633 nm and 40°C. The transmissive homogenous cell gap is *d*=3.33 μm.

		Rise time (ms)								
		1	**2**	**3**	**4**	**5**	**6**	**7**	**8**	**9**
Decay time (ms)	**1**	*	46.0	30.1	20.2	13.8	10.0	7.61	4.69	2.28
	2	9.81	*	16.3	15.3	11	8.37	5.54	4.04	1.95
	3	9.42	23.4	*	13.3	9.81	7.5	6.56	3.71	1.78
	4	9.01	20.3	15.4	*	9.27	7.15	5.51	3.43	1.64
	5	8.89	18.6	14.7	11.6	*	6.62	5.37	3.11	1.5
	6	8.81	17.0	13.9	10.7	7.67	*	4.78	2.91	1.42
	7	8.7	15.9	13.2	9.99	7.25	5.37	*	2.98	1.39
	8	8.54	14.7	12.3	9.31	6.83	5.27	4.65	*	1.40
	9	8.53	13.7	11.7	8.95	6.71	5.37	3.85	2.86	*

3.2 Amplitude modulation with a 90 MTN cell

Our fast-response LC mixtures can also be used for amplitude modulation, such as Google Glass, HoloLens 1 and Magic Leap One. For intensity modulation, 90° MTN cell [5] is commonly used, in which the required $d\Delta n$~240 nm. From Fig. 1, the Δn of our UCF-2 mixture is 0.224 and γ_1/K_{11} is 6.8 ms/μm^2 at 40°C. Thus, the required cell gap is ~1.1 μm. Under such condition, the average gray-to-gray (GTG) response time is ~1 ms, which enables 1 kHz frame rate operation. Such a high frame rate helps to reduce color breakup in field sequential color displays.

4. Photostability

4.1 Blue stability

For a full-color phase-only LCoS devices, red (λ=638 nm), green (λ=524 nm) and blue (λ=448 nm) are the three primary colors. Comparing to the low-energy red and green photons, high-energy blue photons are more detrimental to the LC mixture. Therefore, the lifetime of the LC mixture in practical use is mainly determined by the blue light. In a waveguide-based AR display, the total system's optical efficiency is less than 10%. In order to obtain 1,000 nits display brightness to ensure an acceptable sunlight readability, the light source should have at least 10,000-nits, which corresponds to intensity of 10 mW/cm^2. To investigate the photostability, we chose UCF-2 as an example for this study because of its better electro-optical performance. UCF-2 was injected into a 3.33-μm-thick homogenous cell with SiO_2 alignment layers. To insulate the LC from oxygen and moisture, we sealed the cell with epoxy glue. Then we illuminated the LC cell at 40°C using a Helium-Cadmiun laser (λ=445 nm) whose full width at half maximum (FWHM) is 10 nm. We measured the birefringence and visco-elastic coefficient of the sample every 12 hours or so and recorded the changes. As shown in Fig. 2(a), even after 300 kJ/cm^2 of laser irradiation, no obvious sign of degradation of UCF-2 is observed. Here, 300 kJ/cm^2 represents 8,000 hours of laser exposure at 10,000 nits.

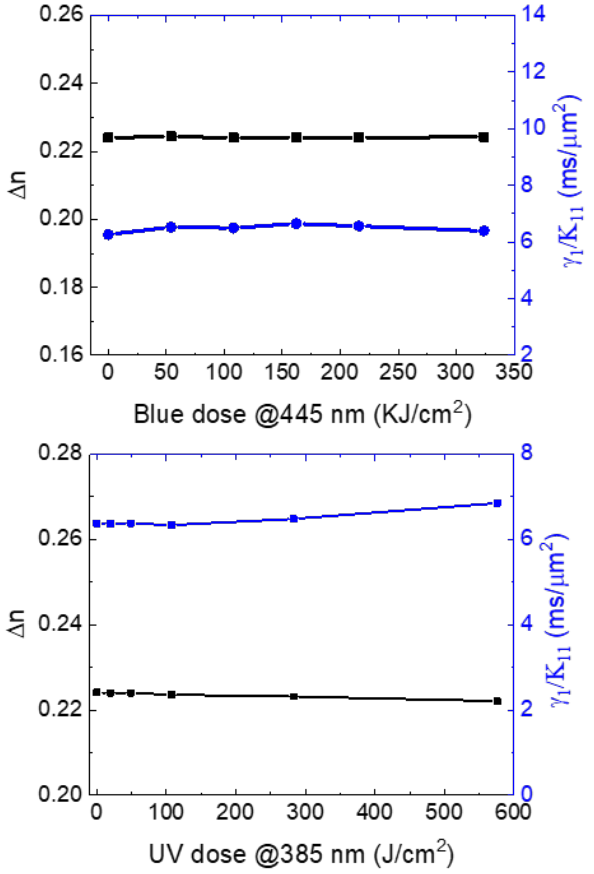

Fig. 2. (a) Measured blue-stability of UCF-2 exposed at 445 nm and 40°C. (b) Measured UV-stability of UCF-2 exposed at 385 nm. The probing laser beam is at λ=633 nm and

measurement temperature is 40°C. Black dots are birefringence and blue dots denote visco-elastic coefficient.

4.2 UV stability

During the fabrication process, in order to seal the filling hole, an LCoS panel is usually exposed to UV light. During the UV exposure, LC mixture or the alignment layer could be damaged, depending on the photostability of employed LC and alignment materials. If a low birefringence LC and inorganic alignment layers were used for LCoS, such as silicon-dioxide (SiO_2), then the photostability is not a concern [11]. However, to achieve fast response time, a low-viscosity and high-birefringence LC mixture is preferred. In order to increase birefringence while keeping a low viscosity, a small percentage (5-10 wt.%) of tolane compounds is often doped to the mixtures. Tolane is sensitive to UV light because of its longer molecular conjugation length.

To evaluate UV stability, we still chose UCF-2 as an example for this study. UCF-2 was injected into an 8.9-μm-thick homogenous cell with SiO_2 alignment layers. We measured the birefringence and visco-elastic coefficient of UCF-2 after long time exposure at 385 nm and recorded the changes in Fig. 2(b). Within the first 100 J/cm^2 of UV dosage, there is almost no change in Δn and γ_1/K_{11}. Since the cell can be sealed within 10 J/cm^2, the liquid crystal would remain stable during the UV sealing process. However, if the UV dosage exceeds ~400 J/cm^2, then the LC material will be degraded gradually.

5. Conclusion

We report two LC mixtures for phase and intensity modulations. The mixtures with high birefringence and relatively large dielectric anisotropy lead to a thin cell gap for achieving 2π phase change under 5V operating voltage. When the mixtures are used in a phase-only LCoS panel, the average phase-to-phase gray level response time is 2.37 ms, which enables 240-Hz refresh rate. On the other hand, if such a LC material is used in the MTN LCoS intensity modulator, the average GTG response time is ~1 ms, which enables 1-kHz frame rate. We believe these mixtures with fast response time, low operating voltage and wide nematic range will find widespread applications for AR and head-up displays.

6. Acknowledgments

The authors are indebted to Ran Chen for technical support and helpful discussion.

7. Reference

1. D. Armitage, I. Underwood, and S. T. Wu, *Introduction to Miscrodisplays* (John Wiley & Sons, 2006).
2. D. Cuypers, H. De Smet, and A. Van Calster, "VAN LCOS Microdisplays: A decade of technological evolution," J. Disp. Technol. 7(3), 127–134 (2011).
3. J. Christmas and N. Collings, "Realizing automotive holographic head up displays," SID Int. Symp. Digest Tech. Papers 47(1), 1017–1020 (2016).
4. Z. Luo, F. Peng, H. Chen, M. Hu, J. Li, Z. An, and S. T. Wu, "Fast-response liquid crystals for high image quality wearable displays," Opt. Mater. Express 5(3), 603–610 (2015).
5. S. T. Wu and C. S. Wu, "Mixed-mode twisted nematic liquid crystal cells for reflective displays," Appl. Phys. Lett. 68, 1455–1457 (1996).
6. M. F. Schiekel and K. Fahrenschon, "Deformation of nematic liquid crystals with vertical orientation in electrical fields," Appl. Phys. Lett. 19, 391–393 (1971).
7. H. Chen, F. Gou, and S. T. Wu, "Submillisecond-response nematic liquid crystals for augmented reality displays," Opt. Mater. Express 7(1):195–201 (2017).
8. I. Haller, "Thermodynamic and static properties of liquid crystals," Prog. Solid State Chem. 10(2), 103–118 (1975).
9. S. T. Wu, "Birefringence dispersions of liquid crystals," Phys. Rev. A 33(2), 1270–1274 (1986).
10. S. T. Wu and C. S. Wu, "Rotational viscosity of nematic liquid crystals A critical examination of existing models," Liq. Cryst. 8(2), 171–182 (1990).
11. C. H. Wen, S. Gauza, and S. T. Wu, "Photostability of liquid crystals and alignment layers," J. Soc. Inf. Disp. 13(9), 805–811 (2005).